P2.3

# RAIN AND CLOUD OBSERVATION BY 95 GHz CLOUD RADAR AND 13.8GHZ PRECIPITATION RADAR

Suginori Iwasaki*
Frontier Observational Research System for Global Change, Yokohama, Japan
Hiroshi Hanado, Hiroaki Horie, Hiroshi Kuroiwa, Hiroshi Kumagai
Communications Research Laboratory, Tokyo, Japan
Hajime Okamoto
Tohoku University, Sendai, Japan

ABSTRACT

We have rain and cloud with precipitation observations by using 13.8 GHz precipitation radar (CAMPR) and 95 GHz cloud radar (SPIDER) at Kashima city, Japan, in November of 2000. Melting layers have strong radar echo at a height of 4.5 km for CAMPR, while, those are weak for SPIDER. We also roughly estimate the median of raindrop size distribution and it becomes about 1.7 mm at a melting layer and this is the largest value in that vertical profile.

## 1. INTRODUCTION

Received power by radar depends on the several micro-physical properties of scatters, i.e., size, number concentration, shape and alignment of raindrop and cloud particles. In order to retrieve these micro-physics, synergy observations are effective. Kumagai et al. (1993) and Meneghini and Kumagai (1994) used 10 GHz and 34 GHz airborne radar to observe rain in the western Pacific. Nakamura et al. (1990) had ground-based rain observations by use of 5.3 GHz, 10 GHz, 34 GHz, and 14 GHz radar. However, their radars are not suitable to observe the cloud because of their wavelengths. Thus, we use 13.8 GHz precipitation radar, CAMPR (Kumagai et al. 1996) and 95 GHz cloud radar, SPIDER (Horie et al. 2000) to observe rain and cloud with precipitation in February and November, 2000. The advantage of this study is to be able to observe the detail of the cloud and to know the relation between cloud and rain because 95 GHz cloud radar has sensitivity for cloud particles.

In section 2, we show our rain observation results by CAMPR and SPIDER. In section 3 and 4, we roughly estimate the raindrop size.

* Corresponding author address: Suginori Iwasaki, FORSGC, 3173-25 shouwa-machi, Kanazawa, Yokohama 236-0001, Japan; e-mail: iwasaki@jamstec.go.jp.

## 2. OBSERVATION

In this section, we introduce our radar system and the results of the rain and cloud synergy observation.

13.8 GHz precipitation radar (CAMPR) and the disdrometer are co-located at Kashima city, Japan, and 95 GHz cloud radar (SPIDER) is also located about 500 m far from these two systems. CAMPR is calibrated by the disdrometer. In order to calibrate SPIDER, we fit the equivalent radar reflectivity factor Ze (Doviak and Zrnuc 1993) measured by SPIDER into that by CAMPR for the thin cloud observations. Because scattering properties of both wavelengths are Rayleigh scattering, it is expected Ze for CAMPR and that for SPIDER become same value.

Figs. 1 show the equivalent radar reflectivity factor in decibel unit dBZe by rain and cloud with precipitation observed at Kashima city on 2 November,

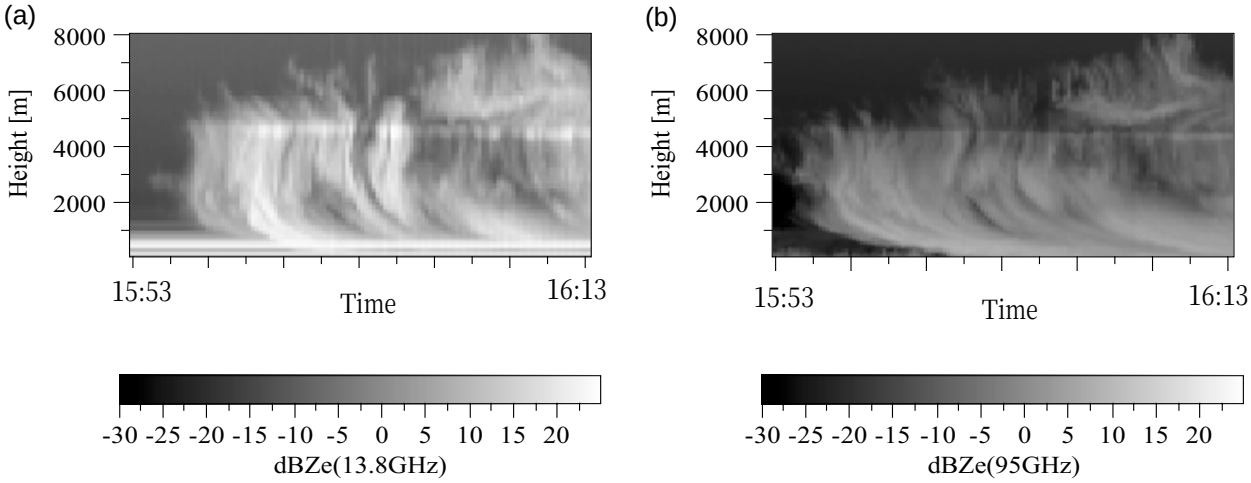


Fig. 1: Equivalent radar reflectivity factor by rain observed at Kashima city on 2 November, 2000 for the period of 15:53-16:13. (a) 13.8 GHz precipitation radar (CAMPR) and (b) 95 GHz cloud radar (SPIDER). Vertical axis denotes the height [m], and horizontal axis denotes time. Both radar observed in zenith direction.

2000 for the period of 15:53-16:13. Fig. 1a is dBZe for CAMPR and Fig. 1b is dBZe for SPIDER. Both of them observe in zenith direction. Melting layers have strong radar echo at a height of 4.5 km for CAMPR, while, those are weak for SPIDER especially around 16:00. Please note that data less than a height of 2 km are not valid because of the radar system problem.

### 3. ESTIMATION OF THE RAINDROP SIZE DISTRIBUTION

In this section, we introduce our computation method to retrieve size distribution of the raindrops. At first, we assume that the drop size distribution is the exponential distribution

$$\frac{dN}{dD} = N_0 \exp(-\Lambda D) \qquad (1)$$

where D denotes a diameter of the particles, and drop concentration $N_0$ and the exponential slope $\Lambda$ are parameters. We use Mie theory to calculate the backscattering cross section and extinction cross section (Bohren and Huffman 1998).

Fig. 2 shows the relation between dBZe for CAMPR (dBZc) and that for SPIDER (dBZs). Each curve denotes the different $N_0$ and $\Lambda$. We assume that optical constants of scatters are that of liquid water at a temperature of 0 deg. (Ulaby et al. 1986). It shows that dBZc and dBZs are not the same value because the scattering by the particles larger than 100 μm is beyond Rayleigh scattering region for SPIDER, while that for CAMPR is still within Rayleigh scattering region. Therefore, when dBZc and dBZs are given, $N_0$ and $\Lambda$ are derived.

Next we calculate $N_0$ and $\Lambda$ for each range bin n. In step (1) and (2), we calculate the radar attenuation from radar to scatters at range bin number n. Next we compute backscattering coefficient $\sigma_{bk}(r)$ and extinction coefficient $\sigma_{ext}(r)$ at a height of r in step (3).

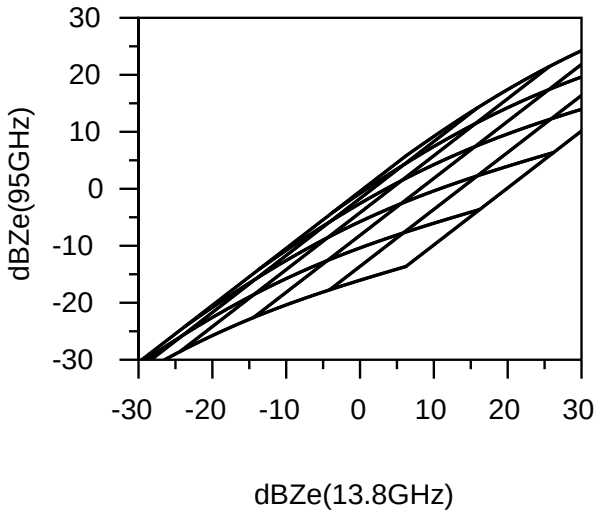


Fig. 2 Relation between the equivalent radar reflectivity factor in decibel unit for CAMPR (dBZc) and that for SPIDER (dBZs). Each curve denotes the different $N_0$ and $\Lambda$. We assume that scatters are liquid water at a temperature of 0 deg..

(Step 1) We define the normalize received power p(r) as Eq. (2) where r is a distance between radar and scatters. *m* is an optical constant of the scatter and λ denotes the wavelength of interest. Thus, p(r) is derived from Ze exp(-2$\sigma_{ext}$r) measured by the radar observations. p(r) is also derived from the theoretical computations when $\sigma_{bk}$(r) and $\sigma_{ext}$(r) are given.

$$p(r) \equiv \frac{\sigma_{\mathrm{bk}}(r)}{r^2}\exp\left(-2\sigma_{\mathrm{ext}}r\right) \equiv \frac{\pi^5}{\lambda^4}\left|\frac{m^2-1}{m^2+2}\right|^2 \frac{Z_{\mathrm{e}}(r)}{r^2}\exp\left(-2\sigma_{\mathrm{ext}}r\right) \quad (2)$$

(Step 2) Then we define the averaged logarithm of p(r), <ln P>$_n$ (see Eq. 3). <ln P>$_{n,obs}$ in Eq. 3a is calculated by the observational results. <ln P>$_{n,cal}$ in Eq. 3b is calculated by the theoretical computations.

$$\left\langle \ln P^{\mathrm{obs}} \right\rangle_n = \frac{1}{n}\sum_{i=1}^{i=n} \ln p^{\mathrm{obs}}(i) \quad (3a)$$

$$\left\langle \ln P^{\mathrm{cal}}(r_{\mathrm{n}}) \right\rangle = \frac{1}{r_n - r_0}\left( \ln\left\langle \sigma_{\mathrm{bk}} \right\rangle \int_{r_0}^{r_n} dr - 2\int_{r_0}^{r_n} drr \right) - 2\left\langle \sigma_{\mathrm{ext}} \right\rangle \frac{1}{r_n - r_0}\int_{r_0}^{r_n} drr \quad (3b)$$

Then we choose <$\sigma_{bk}$>$_n$ and <$\sigma_{ext}$>$_n$ to fit <ln P>$_{n,cal}$ into <ln P>$_{n,obs}$.

(Step 3) We calculate $\sigma_{bk}$(r) and $\sigma_{ext}$(r) for each range bin by using <$\sigma_{ext}$>$_n$ and Eq. (4). Because $\sigma_{bk}$(r) and $\sigma_{ext}$(r) are calculated by $N_0$ and Λ, we derive $N_0$ and Λ.

$$p^{\mathrm{cal}}(r_{n+1}) \approx \frac{1}{\Delta r}\int_{r_{n+1}-\Delta r/2}^{r_{n+1}+\Delta r/2} dr \frac{\sigma_{bk}}{r^2} \times \exp\left\{-2\left[\left\langle \sigma_{\mathrm{ext}} \right\rangle_{\mathrm{n}}\left(r_{\mathrm{n+1}} - \Delta r/2\right)\right]\right\} \times \exp\left(-2\int_{r_{n+1}-\Delta r/2}^{r} dh\sigma_{\mathrm{ext}}\right) \quad (4)$$

The advantage of this method is that it never induces the accumulative error because we do not use the results of the step (4) for the other calculations. The attenuation for SPIDER is large, and it is about 2.7 dB/km for the rain rate 1 mm/h assumed Marshall-Palmer distribution so the accumulative error make a fatal error. Thus, we need to avoid this error. The disadvantage of this method is that we assume that ln $\sigma_{bk}$ is almost constant not to make a significant error to solve <$\sigma_{ext}$>$_n$. Thus, this method is not solved for every rain observation.

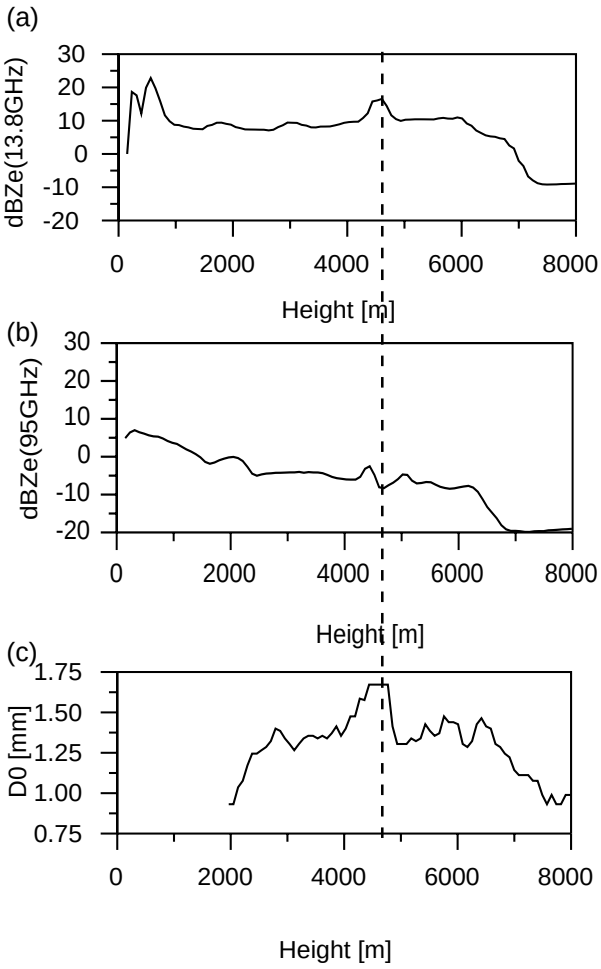


Fig. 3: Vertical profiles of the equivalent radar reflectivity factor in decibel unit for CAMPR (a) and that for SPIDER (b), at 16:13 in Fig. 2. (c) the same as (a) but the median of the size distribution $D_0$ retrieved from (a) and (b). Vertical axis denotes a height [m]. Dotted line denotes the same height.

## 4. SIMULATION

In this section, we show the numerical results for the section 3. Figs. 3 are the vertical profiles of the dBZe for CAMPR (a) and that for SPIDER (b), at 16:13 in Fig. 2. Fig. 3(c) is the same as Fig. 3(a) but the median of the size distribution $D_0$ defined as Eq. 5.

$$D_0 = \frac{3.67}{\Lambda} \quad (5)$$

It is clear that the melting layer becomes a bright band at a height of 4.5 km for CAMPR, and the value is about 16 dBZe. However, melting layer for SPIDER becomes dark band. This is the same results as the light rain observation by lidar (Sassen and Chen, 1995). Therefore, some particles in melting

layer might be large enough and their scattering property is within geometrical optics region for SPIDER. Fig. 3(c) shows that $D_0$ becomes 1.7 mm at a melting layer and it is a largest value in this vertical profile. Although we assume that every scatters are water and our computation is limited (see section 3), it derives a reasonable result.

## 5. Summary

We have synergy rain and cloud with precipitation observation by using 13.8 GHz precipitation radar (CAMPR) and 95 GHz cloud radar (SPIDER) in February and November, 2000. We show that melting layers have strong radar echo for CAMPR, while, those are weak for SPIDER. We also roughly estimate the raindrop size, and the median of the raindrop size distribution becomes 1.7 mm around melting layer.

Because our computation is limited to apply for every rain observation, we are now intensively developing our method. We will report the general method in near future.

## REFERENCES


Bohren C. F. and D. R. Huffman, 1998; *Absorption and Scattering of Light by Small Particles*, Wiley, New York.

Doviak R. J., and D. S. Zrnuc, 1993; *DOPPLER RADAR AND WEATHER OBSERVATIONS*, Academic Press.

Horie H., T. Iguchi, H. Hanado, H. Kuroiwa, H. Okamoto, and H. Kumagai, 2000; Development of a 95-GHz Airborne Cloud Profiling Radar (SPIDER), *IEICE Trans. Commun.*, E89-B, 2010-2020.

Kumagai H., and R. Meneghini 1993; Preliminary Results from Multiparameter Airborne Rain Radar Measurement in the Western Pacific., *J. Appl. Meteor*, **32**, 431-440.

Kumagai, H., K. Nakamura, H. Hanado, K. Okamoto, N. Hosaka, N. Miyano, T. Kozu, N. Takahashi, T. Iguchi, and H. Miyauchi, 1996; CRL Airborne Multiparameter Precipitation Radar (CAMPR): System Description and Preliminary Results, *IEICE Trans. Commun.*, **E79-B**, 770-778.

Meneghini R. and H. Kumagai, 1994; Characteristics of the Vertical Profiles of Dual-Frequency, Dual-Polarization Radar Data in Stratiform Rain., *J. Atmos. Oceanic Technol.*, **11**, 701-711.

Nakamura K., H. Inomata, T. Kozu, J. Awaka, and K. Okamoto 1990; Rain Observation by an X- and Ka-band Dual-Wavelength Radar., *J. Meteor. Soc. Japan*, **68**, 509-521.

Sassen K., and T. Chen, 1995; The lidar dark band: Am oddity of the radar bright band analogy, *Geoph. Res. Lett.*, **22**, 3505-3508.

Ulaby, F. T., R. K. Moore, and A. K. Fung, 1986; *MICROWAVE REMOTE SENSING ACTIVE AND PASSIVE, volume III, From Theory to Applications*, Artech house, Inc..